JACS
JOURNAL OF THE AMERICAN CHEMICAL SOCIETY

COMMUNICATION

pubs.acs.org/JACS

Thieno[3,2-*b*]thiophene−Diketopyrrolopyrrole-Containing Polymers for High-Performance Organic Field-Effect Transistors and Organic Photovoltaic Devices

Hugo Bronstein,[*,†] Zhuoying Chen,[*,‡] Raja Shahid Ashraf,[†] Weimin Zhang,[†] Junping Du,[†] James R. Durrant,[†] Pabitra Shakya Tuladhar,[†] Kigook Song,[§] Scott E. Watkins,[∥] Yves Geerts,[⊥] Martijn M. Wienk,[#] Rene A. J. Janssen,[#] Thomas Anthopoulos,[†] Henning Sirringhaus,[‡] Martin Heeney,[†] and Iain McCulloch[†]

[†]Imperial College London, London SW7 2AZ, U.K.

[‡]Cavendish Laboratory, University of Cambridge, J. J. Thompson Avenue, Cambridge CB3 0HE, U.K.

[§]Kyung Hee University, Yongin, Gyeonggi-do 446-701, Korea

[∥]CSIRO Materials Science and Engineering, VIC 3169, Australia

[⊥]Université Libre de Bruxelles, 1050 Bruxelles, Belgium

[#]Eindhoven University of Technology, P.O. Box 513, 5600 MB Eindhoven, The Netherlands

Supporting Information

ABSTRACT: We report the synthesis and polymerization of a novel thieno[3,2-*b*]thiophene−diketopyrrolopyrrole-based monomer. Copolymerization with thiophene afforded a polymer with a maximum hole mobility of 1.95 $cm^2 V^{-1} s^{-1}$, which is the highest mobility from a polymer-based OFET reported to date. Bulk-heterojunction solar cells comprising this polymer and $PC_{71}BM$ gave a power conversion efficiency of 5.4%.

There is considerable interest in the synthesis of narrow-band-gap conjugated polymers for use in organic photovoltaic (OPV) and organic field-effect transistor (OFET) devices. Their solution processability and mechanical properties allow access to a new generation of cheap and flexible transistors and solar devices. Current state of the art polymeric materials have allowed for the fabrication of OFETs with mobilities of ~1 $cm^2 V^{-1} s^{-1}$ [1] and OPV devices with power conversion efficiencies (PCEs) of over 7%.[2]

Diketopyrrolopyrrole (DPP)-based copolymers have emerged as extremely attractive materials for both thin-film transistors and solar cell devices in recent years. The DPP core's electron-deficient nature has been exploited for the synthesis of extremely narrow band gap donor−acceptor-type materials that are well-suited for use in OPVs with high PCEs reported from both small molecules and polymers.[3−6] Furthermore, the planarity of the DPP skeleton and its ability to accept hydrogen bonds (and other types of electrostatic interactions) result in copolymers that encourage $\pi-\pi$ stacking. Typically, these DPP-based copolymers are prepared via either Suzuki or Stille coupling of the 3,6-bis(5-bromothiophen-2-yl)-2,5-dialkylpyrrolo[3,4-*c*]pyrrole-1,4-(2*H*,5*H*)-dione core with the desired comonomer, which as a result means that the electron-deficient DPP unit is always flanked by two thiophenes. Variation of the comonomer has yielded polymers with extremely attractive properties for both OPV and OFET devices. For instance, copolymerization with thiophene derivatives or benzothiadiazole resulted in polymers with impressive ambipolar charge-carrier mobilities.[7,8] Recently, a copolymer of 3,6-bis(5-bromothiophen-2-yl)-*N*,*N*′-bis(2-octyl-1-dodecyl)-1,4-dioxopyrrolo[3,4-*c*]pyrrole and 2,5-bis(trimethylstannyl)thieno[3,2-*b*]thiophene showed an impressive hole mobility of ~0.9 $cm^2 V^{-1} s^{-1}$.[9] In terms of materials for OPVs, copolymerization of the same DPP monomer (albeit having a slightly different solubilizing alkyl chain) with phenylene-1,4-diboronic acid bispinacol ester afforded a polymer that was used to fabricate OPV devices with efficiencies of ~5.5%.[10]

Despite the significant number of reports on DPP-based copolymers, there have been very few studies on the effect of modifying the 3,6-bis(5-bromothiophen-2-yl)-2,5-dialkylpyrrolo-[3,4-*c*]pyrrole-1,4-(2*H*,5*H*)-dione monomer. One very recent example was the replacement of the flanking thiophenes by furans, which resulted in polymers with high PCEs in solar cell devices.[11] We were interested in increasing the intermolecular association of DPP-based copolymers by replacing the

Scheme 1. Synthesis of Novel DPP Polymers

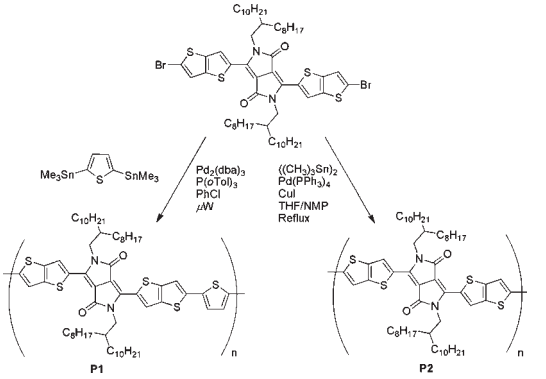

Received: November 25, 2010
Published: February 18, 2011

   dx.doi.org/10.1021/ja110619k | *J. Am. Chem. Soc.* 2011, 133, 3272–3275

Table 1. Properties of Polymers P1 and P2

polymer	M_n (kDa)[a]	M_w (kDa)[a]	PDI[a]	λ_{max} (nm) soln.[b]	λ_{max} (nm) film[c]	HOMO (eV)[d]	LUMO (eV)[e]
P1	14	75	5.4	812	746, 795	−5.06	−3.68
P2	16	78	4.9	857	784	−5.04	−3.76

[a] Determined by GPC using polystyrene standards and PhCl as the eluent. [b] Measured in dilute chloroform solution. [c] Spin-coated from 5 mg/mL PhCl solution. [d] Measured by UV−PES. [e] Estimated by addition of the absorption onset to the HOMO.

thiophenes with larger thieno[3,2-*b*]thiophene units, which have been used extensively in many materials with high charge-carrier mobilities.[12] The thienothiophene units extend the polymer coplanarity and also promote a more delocalized HOMO distribution along the backbone, which we expect to enhance intermolecular charge-carrier hopping. Our approach to the inclusion of thieno[3,2-*b*]thiophene units was to synthesize a novel DPP-based monomer unit bearing the fused heterocycles and use this as the basis for novel copolymers. This would allow the synthesis of a polymer with a greater number of thieno[3,2-*b*]thiophene units than would be accessible using the standard thiophene-flanked DPP monomer.

The synthesis of the novel monomer 3,6-bis(2-bromothieno-[3,2-*b*]thiophen-5-yl)-2,5-bis(2-octyldodecyl)pyrrolo[3,4-*c*]-pyrrole-1,4-(2*H*,5*H*)-dione was achieved using reactions analogous to those of the commonly used 3,6-bis(5-bromothiophen-2-yl)-2,5-dialkylpyrrolo[3,4-*c*]pyrrole-1,4-(2*H*,5*H*)-dione; the procedure is described in detail in the Supporting Information (SI). A long, branched hydrocarbon chain was chosen to ensure maximum solubility.

The synthesis of the polymers is shown in Scheme 1. The thiophene copolymer **P1** was synthesized under standard microwave Stille coupling conditions[13] in chlorobenzene, whereas the homopolymer **P2** was synthesized using a Stille-like homopolymerization procedure. The polymers were purified by precipitation into methanol followed by Soxhlet extraction using acetone, hexane, and finally chloroform. Residual catalytic metal impurities were removed by heating and vigorous stirring of a chloroform solution of the polymeric material in the presence aqueous sodium diethyldithiocarbamate.[14] Satisfactory molecular weights were obtained in both cases, but because of the extremely low solubility of the materials in acetone and hexane, removal of lower-molecular-weight oligomers was problematic, as indicated by the moderately low number-average molecular weights (M_n = 14 and 16 kDa for **P1** and **P2**, respectively) and high polydispersity indexes (PDIs) (Table 1; also see section S3 in the SI). Furthermore, accurate determination of the molecular weight of DPP-based copolymers is often problematic, as aggregation is commonly observed in solution, which can result in an overestimation of the molecular weight.[10] To avoid this, the gel-permeation chromatography (GPC) measurements were performed at the lowest possible dilution while maintaining a reasonable signal-to-noise ratio.

In dilute chloroform solution, both polymers display absorption maxima at greater than 800 nm with a shoulder at a shorter wavelength (Figure 1). This feature is more intense in homopolymer **P2**. It is unclear whether the shoulder is the result of lower-molecular-weight oligomers present in the sample that have not reached their maximum effective conjugation length, a vibronic shoulder arising from polymer aggregates in solution, or merely a spectral feature of the polymer chain.

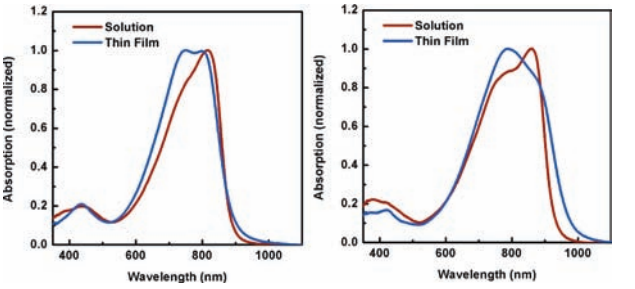

Figure 1. Solution (chloroform) and thin-film (from chlorobenzene) UV−vis absorption spectra of (left) **P1** and (right) **P2**.

In the solid state (films spin-coated from chlorobenzene solution, 5 mg/mL), **P2** shows a significant red shift (∼50 nm) in its absorption onset, which can be attributed to solid-state packing effects, whereas for **P1**, this increase is much smaller (∼20 nm). Unusually, the absorption maxima for both polymers are blue-shifted relative to the solution measurement, a result of what appears to be the shorter-wavelength shoulder increasing in intensity and becoming the dominant feature.

The HOMO energy levels of the polymers were measured by photoelectron spectroscopy in air (PESA), and the two polymers gave similar values of around −5.05 eV. The LUMO was estimated by addition of the thin-film optical band gap (absorption onset) to the HOMO, which gave values of −3.68 eV for **P1** and −3.76 eV for **P2**. The tendency for DPP-containing copolymers to aggregate in the solid state implies that the values obtained for the frontier-orbital energy levels cannot be taken as absolute. The choice of solvent and concentration of a spin-coated film can greatly affect the morphology of these materials and as a result can affect both UV−PES and UV−vis measurements.

Top-gate/bottom-contact OFETs with gold source/drain electrodes (Figure 2b) were used to test the ambipolar mobilities of polymers **P1** and **P2**. Ambipolar charge-transport characteristics were observed in both **P1**- and **P2**-based OFETs studied in this work. Even though the effective saturation field-effect mobilities of these polymers are gate-voltage-dependent, remarkably high hole mobilities of 1−2 $cm^2\ V^{-1}\ s^{-1}$ were typically observed in **P1**-based OFETs. These can be compared with results for the analogous poly(diketopyrrolopyrrole−terthiophene) (i.e., the more common thiophene-flanked DPP core copolymerized with thiophene), which has an as-spun hole mobility of 0.04 $cm^2\ V^{-1}\ s^{-1}$ (although it should be mentioned that this polymer has linear hexadecyl solubilizing groups).[4]

Figure 2a displays the typical transistor transfer characteristics of as-spun **P1** and as-spun **P2** OFETs (channel length L = 20 um, channel width W = 1 cm) at different source−drain voltages (V_{ds}). From the slopes obtained by linear fitting of plots of the square-root of the drain current versus the gate voltage (V_g) for V_g ranging from −68 to −78 V for holes and 6 to 16 V for

dx.doi.org/10.1021/ja110619k |*J. Am. Chem. Soc.* 2011, 133, 3272–3275

electrons, the **P1** OFET data shown in Figure 2a yield effective saturation hole and electron mobilities of 1.95 and 0.03 $cm^2 V^{-1} s^{-1}$, respectively. In comparison with **P1**, **P2**, which has a similar chemical structure except that the thiophene moiety in its repeat unit is absent, showed modest hole mobilities but higher electron mobilities in our OFET studies (Table 2). The highest mobilities were extracted from the transfer characteristics with V_{ds} = −100 V (Figure S4.1 in the SI). The gate-voltage-dependent mobilities found in this study are not uncommon in the field of solution-processed OFETs.[15−18] This phenomenon was found to originate from charge-density-dependent mobilites[16] and has often been attributed to the existence of disorder[15] or the presence of traps.[17,18] For both materials, the ambipolar mobilities were most optimized on as-spun polymer films. In addition to as-spun films, we also studied annealed polymer films at 240 and 320 °C for OFET applications. However, devices based on annealed films of these materials did not show any mobility improvements in comparison with as-spun films (Figure S4.2). Because of the energy offset between the work function of gold and the LUMO levels of these polymers, the electron transport in both the **P1** and **P2** OFETs was injection-limited, as shown by the output characteristics at low V_{ds} (Figure 2d). For both polymers, hysteresis was observed in the output characteristics at high gate voltages, which may due to the existence of charge-trapping impurities or defects in the polymer or at the interface. Contacts without oxygen plasma treatment did not improve the device performance (Figure S4.3). By further optimization of the polymer molecular weights and the source and drain contacts, OFETs based on these polymers could yield even higher field-effect mobilites.[19]

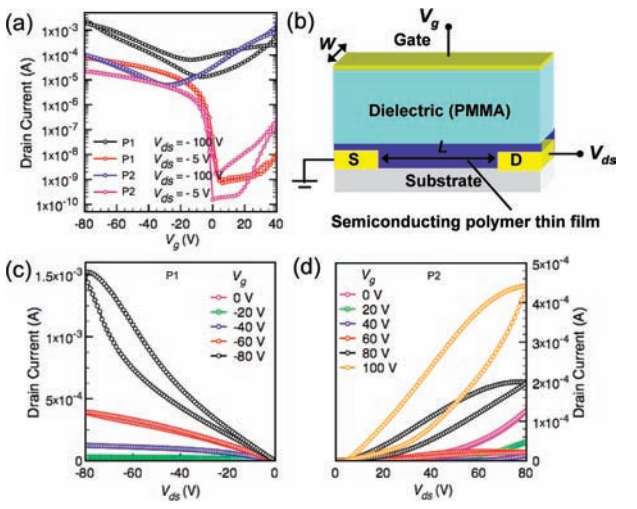

Figure 2. (a) Transfer characteristics of a typical OFET devices based on as-spun **P1** and as-spun **P2** polymer thin films. For the **P1** OFET, the effective hole mobility of 1.95 $cm^2 V^{-1} s^{-1}$ and electron mobility of 0.03 $cm^2 V^{-1} s^{-1}$ in the saturation regime were calculated from the slopes obtained by linear fitting of plots of the square-root of the drain current vs V_g for V_g ranging from −68 to −78 V for holes and 6 to 16 V for electrons. (b) Schematic of the top-gate/bottom-contact transistor structure used in this study. (c) The p-channel output characteristics of the **P1**-based OFET whose transfer characteristics are shown in (a). (d) The n-channel output characteristics of the **P2**-based OFET whose transfer characteristics are shown in (a). All of the OFETs for which data are shown in this figure were fabricated with channel length L = 20 μm, channel width W = 1 cm, and ∼550 nm thick PMMA as the gate dielectric (capacitance C_i = 6.2 nF cm^{-2}).

It is interesting to note the large difference in the hole mobilities of the two materials despite their structural similarity. It is suggested that the reduced distance between the solubilizing alkyl chains in **P2** results in increased steric interactions that could affect the nature of the polymer packing in the solid state. The large red shift in the absorption spectra of **P2** relative to **P1** would suggest that the polymer chains pack in different manners. The nature of the solid-state packing has been found to profoundly influence the charge-carrier mobility of conjugated polymer.[12] Initial X-ray diffraction and differential scanning calorimetry studies of both polymers in their as-spun conditions have not shown any evidence of crystallinity. Investigations into the solid-state structures of these materials will be presented separately.

OPV devices were fabricated with polymers **P1** and **P2** by spin-coating of a 1:2 polymer/$PC_{71}BM$ mixture in a 4:1 chloroform/*o*-dichlorobenzene (ODCB) solution onto an ITO:PEDOT substrate followed by evaporation of LiF/Al as a back-contact. The two materials displayed similar open-circuit voltages (V_{oc}) of ∼0.57 V (Table 3). Devices based on **P2** gave satisfactory short-circuit currents (J_{sc}) of ∼9 mA cm^{-2} (Figure 3), resulting in a PCE of ∼3%. **P1** devices, however, had a remarkable J_{sc} of ∼15 mA cm^{-2}, which, in combination with a high fill factor (0.61), gave a PCE of 5.4%. The superior performance of **P1** over **P2**, despite its reduced absorption range, could be attributed to several factors. It could be the result of a more favorable morphology, as it was already observed that there is clearly a difference in the solid-state packing effects in neat films of the two materials. This could be a result of the reduced distance between the two DPP repeat units as mentioned previously, which could in turn reduce the amount of fullerene intercalation that can occur; this is a factor that has been shown to affect the optimal donor/acceptor ratio in other systems.[20] However, we believe that the slightly lower LUMO level of **P2** may be too close in energy to that of the fullerene acceptor, which can result in less efficient charge separation. Unfortunately, because of the aforementioned issue with accurately measuring

Table 3. OPV Device Characteristics of P1- and P2-Based Solar Cells

polymer	J_{sc} (mA cm^{-2})	V_{oc} (V)	FF	PCE (%)
P1	15.0	0.58	0.61	5.4
P2	8.9	0.57	0.59	3.0

Table 2. OFET Properties of As-Spun P1 and P2 Polymers[a]

polymer	μ_{hole} ($cm^2 V^{-1} s^{-1}$)	I_{on}/I_{off} for holes	$V_{th,lin,hole}$ (V)	$\mu_{electron}$ ($cm^2 V^{-1} s^{-1}$)	I_{on}/I_{off} for electrons	$V_{th,lin,electron}$ (V)
P1	1.42 ± 0.46	∼10^5	∼0	0.063 ± 0.008	10^3−10^4	∼56
P2	0.037 ± 0.015	∼10^5	∼ −5	0.30 ± 0.094	10^4−10^5	∼42

[a] μ_{hole} and $\mu_{electron}$ refer to the highest effective mobilities measured in the saturation regime for a gate-voltage range of 10 V. The threshold voltages ($V_{th,lin}$) and the on-to-off ratios (I_{on}/I_{off}) were extracted from the linear regime (V_{ds} = −5 V for holes, and V_{ds} = 5 V for electrons). The **P1** and **P2** OFET mobilities reported in this table are averages of five (**P1**) and four (**P2**) devices (L = 20 μm and W = 1 cm), and the error bars denote standard deviations.

dx.doi.org/10.1021/ja110619k |*J. Am. Chem. Soc.* 2011, 133, 3272–3275

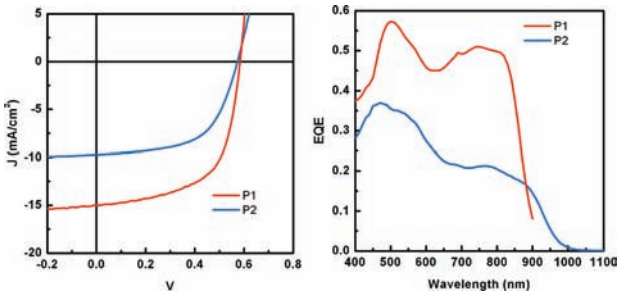

Figure 3. OPV device characteristics of **P1** and **P2**. (left) Current–voltage curves of polymer/$PC_{71}BM$ devices spin-coated from a $CHCl_3$/ODCB mixture. (right) External quantum efficiencies of the devices.

the HOMO and LUMO levels of DPP-containing materials, there is not currently enough evidence to confirm this hypothesis.

In conclusion, we have prepared a novel DPP-based monomer containing flanking thieno[3,2-*b*]thiophenes that upon copolymerization with thiophene affords a polymer with hole mobilities of almost 2 $cm^2\ V^{-1}\ s^{-1}$ without even the need for high-temperature annealing. To the best of our knowledge, this is the highest-performing polymer-based FET reported to date. The use of the same polymer in an OPV device resulted in a device performance of 5.4%.

■ ASSOCIATED CONTENT

Supporting Information. Synthesis of monomers and copolymers and transistor characteristics. This material is available free of charge via the Internet at http://pubs.acs.org.

■ AUTHOR INFORMATION

Corresponding Author
h.bronstein@imperial.ac.uk

■ ACKNOWLEDGMENT

This work was in part carried out under the EC FP7 ONE-P Project 212311 and DPI Grant 678, with support from the International Collaborative Research Program of Gyeonggi-do, Korea.

■ REFERENCES

(1) Zhang, W.; Smith, J.; Watkins, S. E.; Gysel, R.; McGehee, M.; Salleo, A.; Kirkpatrick, J.; Ashraf, S.; Anthopoulos, T.; Heeney, M.; McCulloch, I. *J. Am. Chem. Soc.* **2010**, *132*, 11437–11439.
(2) Liang, Y.; Yu, L. *Acc. Chem. Res.* **2010**, *43*, 1227–1236.
(3) Wienk, M. M.; Turbiez, M.; Gilot, J.; Janssen, R. A. J. *Adv. Mater.* **2008**, *20*, 2556–2560.
(4) Bijleveld, J. C.; Zoombelt, A. P.; Mathijssen, S. G. J.; Wienk, M. M.; Turbiez, M.; de Leeuw, D. M.; Janssen, R. A. J. *J. Am. Chem. Soc.* **2009**, *131*, 16616–16617.
(5) Zhou, E. J.; Wei, Q. S.; Yamakawa, S.; Zhang, Y.; Tajima, K.; Yang, C. H.; Hashimoto, K. *Macromolecules* **2010**, *43*, 821–826.
(6) Ashraf, R. S.; Chen, Z.; Leem, D. S.; Bronstein, H.; Zhang, W.; Schroeder, B.; Geerts, Y.; Smith, J.; Watkins, S.; Anthopoulos, T. D.; Sirringhaus, H.; de Mello, J. C.; Heeney, M.; McCulloch, I. *Chem. Mater.* **2011**, *23*, 768–770.
(7) Nelson, T. L.; Young, T. M.; Liu, J.; Mishra, S. P.; Belot, J. A.; Balliet, C. L.; Javier, A. E.; Kowalewski, T.; McCullough, R. D. *Adv. Mater.* **2010**, *22*, 4617–4621.
(8) Sonar, P.; Singh, S. P.; Li, Y.; Soh, M. S.; Dodabalapur, A. *Adv. Mater.* **2010**, *22*, 5409–5413.
(9) Li, Y.; Singh, S. P.; Sonar, P. *Adv. Mater.* **2010**, *22*, 4862–4866.
(10) Bijleveld, J. C.; Gevaerts, V. S.; Di Nuzzo, D.; Turbiez, M.; Mathijssen, S. G. J.; de Leeuw, D. M.; Wienk, M. M.; Janssen, R. A. J. *Adv. Mater.* **2010**, *22*, E242–E246.
(11) Woo, C. H.; Beaujuge, P. M.; Holcombe, T. W.; Lee, O. P.; Fréchet, J. M. J. *J. Am. Chem. Soc.* **2010**, *132*, 15547–15549.
(12) McCulloch, I.; Heeney, M.; Bailey, C.; Genevicius, K.; MacDonald, I.; Shkunov, M.; Sparrowe, D.; Tierney, S.; Wagner, R.; Zhang, W.; Chabinyc, M. L.; Kline, R. J.; McGehee, M. D.; Toney, M. F. *Nat. Mater.* **2006**, *5*, 328–333.
(13) Tierney, S.; Heeney, M.; McCulloch, I. *Synth. Met.* **2005**, *148*, 195–198.
(14) Nielsen, K. T.; Spanggaard, H.; Krebs, F. C. *Macromolecules* **2005**, *38*, 1180–1189.
(15) Shaked, S.; Tal, S.; Roichman, Y.; Razin, A.; Xiao, S.; Eichen, Y.; Tessler, N. *Adv. Mater.* **2003**, *15*, 913–196.
(16) Salleo, A.; Chen, T. W.; Völkel, A. R.; Wu, Y.; Liu, P.; Ong, B. S.; Street, R. A. *Phys. Rev. B* **2004**, *70*, No. 115211.
(17) Dimitrakopoulos, C. D.; Purushothaman, S.; Kymissis, J.; Callegari, A.; Shaw, J. M. *Science* **1999**, *283*, 822–824.
(18) Horowitz, G.; Hajlaoui, M. E.; Hajlaoui, R. *J. Appl. Phys.* **2000**, *87*, 4456–4463.
(19) Tsao, H. N.; Mullen, K. *Chem. Soc. Rev.* **2010**, *39*, 2372–2386.
(20) Mayer, A. C.; Toney, M. F.; Scully, S. R.; Rivnay, J.; Brabec, C. J.; Scharber, M.; Koppe, M.; Heeney, M.; McCulloch, I.; McGehee, M. D. *Adv. Funct. Mater.* **2009**, *19*, 1173–1179.